Formation of partial energy gap below the structural phase transition and the rare-earth element-substitution effect on infrared phonons in *Re*FeAsO (*Re*=La, Nd, and Sm)

T. Dong, Z. G. Chen, R. H. Yuan, B. F. Hu, B. Cheng, and N. L. Wang
Beijing National Laboratory for Condensed Matter Physics, Institute of Physics, Chinese Academy of Sciences, Beijing 100190, China
(Received 5 May 2010; revised manuscript received 16 July 2010; published 26 August 2010)

Single crystals of LaFeAsO, NdFeAsO, and SmFeAsO have been prepared by means of a NaAs flux growth technique and studied by optical spectroscopy measurements. We show that the spectral features corresponding to the partial energy gaps in the spin-density-wave (SDW) state are present below the structural phase transition. This indicates that the electronic state below the structural phase transition is already very close to that in the SDW state. We also show that in-plane infrared phonon modes display systematic shifts toward high frequency upon rare-earth element Nd and Sm substitutions for La, suggesting a strong enhancement of the bonding strength. Furthermore, an asymmetric line shape of the in-plane phonon mode is observed, yielding evidence for the presence of electron-phonon coupling in Fe pnictides.

DOI: 10.1103/PhysRevB.82.054522 PACS number(s): 74.70.Xa, 74.25.Gz, 74.25.nd

I. INTRODUCTION

The discovery of superconductivity at 26 K in F-doped LaFeAsO (Ref. 1) has created tremendous interests in the scientific community. Shortly after this discovery, the superconducting transition temperature T_c was raised beyond 50 K through the substitution of La by rare-earth elements. T_c is found to be 41 K for F-doped CeFeAsO,[2] 52 K for F-doped NdFeAsO,[3] and 55 K for F-doped SmFeAsO.[4] In the so-called 1111 structural type series, the undoped parent compounds were commonly found to have a spin-density-wave (SDW) ground state with a collinear antiferromagnetic spin configuration.[5,6] A structural phase transition occurs prior to the magnetic transition. Because superconductivity appears in the vicinity of the magnetic ordered phase,[6] it is widely believed that the spin fluctuations play a crucial role in the superconducting pairing of electrons while the electron-phonon interactions could not explain the superconductivity in those materials. A theoretical calculation even indicates that the electron-phonon coupling could not lead to the superconductivity with T_c higher than 1 K in those materials.[7]

A critical question here is why the rare-earth element substitutions for La in the 1111 series could significantly enhance the superconducting transition temperature? For La or different rare-earth-based parent compounds, the structural and magnetic phase transitions were found to take place roughly at the same temperatures, then the magnetic interactions should not have much difference. On the other hand, the rare-earth element substitutions lead to certain change in the lattice structure. Some correlations between superconducting transition temperatures and the Fe-As bond length or the Fe-As-Fe angle for the series have been found.[8,9] However, there is still a lack of a complete understanding of the problem. In this work, we performed optical spectroscopy study on single-crystal samples of the several different 1111 compounds, including LaFeAsO, NdFeAsO, and SmFeAsO. We focus our attention on two issues. One is the relationship between the structural and magnetic phase transitions. We identify that the charge excitation gaps have already opened at the structural phase transition, which then discloses the intimate relation between the driving mechanisms of the two transitions. The other is the effect of rare-earth element substitutions on the lattice modes. We found that the in-plane phonon modes display systematic shifts toward high frequency with the substitution of La by Nd and Sm. We also observed asymmetric line shape of the in-plane phonon mode, providing direct evidence for the presence of electron-phonon coupling. The results may imply that the lattice vibrations play some role for the high-temperature superconductivity.

II. EXPERIMENTS AND RESULTS

A. Experiments

The crystal growth in 1111 systems has been proven to be difficult. For a long period, only very small size single crystals could be obtained with typical dimensions less than 300 μm.[10,11] Millimeter-sized single crystals were obtained only by means of NaAs flux technique until recently.[12,13] The *Re*FeAsO (*Re*=La, Nd, and Sm) single crystals used in this study were grown from such a technique and characterized by the x-ray diffractions (XRD) and dc resistivity measurements. For the Sm-based sample, we put 10% F in the initial composition. However the resultant crystals still have a property of the parent compound. The major change is that the resistivity anomaly corresponding to structural transition is suppressed to about 120 K. Detailed descriptions about crystal growth could be found in Ref. 13.

Figure 1 shows the (00l) XRD patterns for the single-crystal samples of *Re*FeAsO (*Re*=La, Nd, and Sm) with Cu $K\alpha$ radiation. The XRD patterns indicate that the samples are of the characteristic of good crystallization along the c axis. The (00l) peaks shift toward higher 2θ angles systematically from LaFeAs to NdFeAsO and SmFeAsO, suggesting a reduction in c-axis lattice parameter. The obtained c-axis lattice parameter is c=8.758 Å for LaOFeAs, 8.595 Å for NdOFeAs, and 8.497 Å for SmFeAsO, respectively. The reduction in the c-axis lattice parameter is apparently due to the smaller ionic radius of the rare-earth elements Nd and Sm. Those values are consistent with earlier lattice parameters determined from the polycrystalline samples.[14]

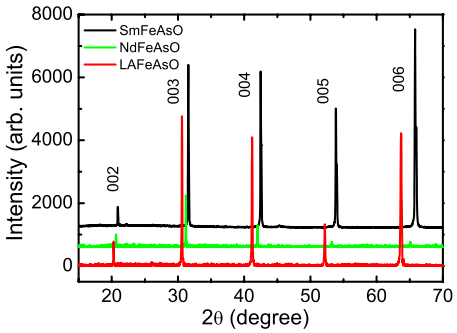

FIG. 1. (Color online) The (00*l*) x-ray diffraction patterns of single-crystals *Re*FeAsO (*Re*=La, Nd, and Sm).

Optical measurement was done on a Bruker IFS 66v/s spectrometer in the frequency range from 40 to 25 000 cm^{-1}. An *in situ* gold and aluminum overcoating technique was used to get the reflectance $R(\omega)$. The real part of conductivity $\sigma_1(\omega)$ is obtained by the Kramers-Kronig transformation of $R(\omega)$.

B. Electronic spectra

Figure 2 shows the optical reflectance and conductivity spectra up to 6000 cm^{-1} of LaFeAsO, NdFeAsO, and SmFeAsO at two representative temperatures 300 K and 10 K, respectively. The data of LaFeAsO were already presented in Ref. 13 where its spectral features and correlation effect were discussed. Here they are used for a purpose of comparison. We can see that all the compounds exhibit similar spectral features in both the paramagnetic and SDW states. At room

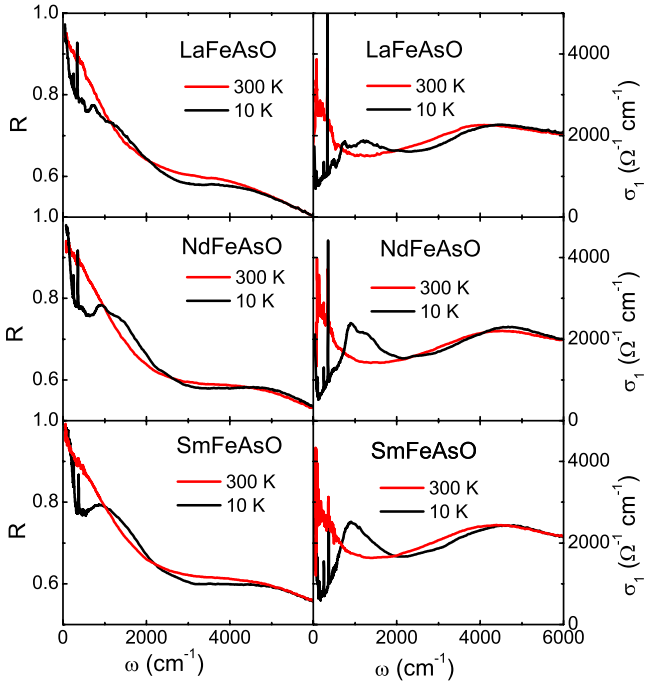

FIG. 2. (Color online) In-plane optical reflectance and conductivity spectra up to 6000 cm^{-1} at 300 and 10 K for La-, Nd-, and Sm-based 1111 single-crystal samples.

temperature, the reflectance $R(\omega)$ drops almost linearly with frequency at low-ω region, then merges into the high values of a background contributed mostly from the interband transitions from the mid-infrared to visible regime. The conductivity spectrum $\sigma_1(\omega)$ displays a Drude-type component at low frequency and a rather pronounced spectral weight in the high frequencies. A broad peak is seen near 4500 cm^{-1}. In the SDW state at 10 K, dramatic spectral change was seen at low frequencies. The reflectance below 1000 cm^{-1} shows a remarkable suppression while it is enhanced between 1000 and 2000 cm^{-1}. Then, in the conductivity spectra, the spectral weight is severely suppressed at low frequencies and the missing spectral weight is transferred to the absorption peaks at high energies. This gives optical evidence for the gap formation on the Fermi surfaces in the SDW state. Since the reflectance still increases fast toward unity at lower frequencies, residual free carriers or Drude component is still left in the magnetic ordered state. Therefore, the Fermi surfaces are not fully gapped below T_N. Those spectral features are also observed in 122-type AFe_2As_2 (A=Ba and Sr) (Ref. 15) and 111-type $Na_{1-\delta}FeAs$ single crystals[16] across the SDW transitions, indicating the generic properties of undoped FeAs-based systems.

As mentioned in the introduction, for 1111 parent compounds, a structural transition from a tetragonal-to-orthorhombic phase occurs prior to the SDW or magnetic transition whereas the two transitions occur simultaneously for 122-type compounds. The relation between the structural and SDW transitions has been a subject of many discussions.[17–20] Theoretically, it was suggested that the structural transition is driven by the magnetic transition.[17–20] Then it is important to detect experimentally whether the charge-excitation gaps open in the structurally distorted phase (above the magnetic transition) or not, an issue which has not been addressed by any of previous optical measurements. For this purpose, we present a detailed temperature-dependent $R(\omega)$ and $\sigma_1(\omega)$ spectra for one of the parent compounds, NdFeAsO.

Similar to other 1111-type compounds, NdFeAsO exhibits a pronounced anomaly in the resistivity $\rho(T)$ near 150 K, below which $\rho(T)$ decreases rapidly with decreasing temperature.[21] Figure 3 shows the temperature dependence of the resistivity $\rho(T)$ of a NdFeAsO single crystal. Compared with the data of polycrystalline samples,[21] the decrease in the resistivity near 150 K is much faster for single-crystal sample. Its temperature derivative, $d\rho(T)/dT$, shows a sharp peak at 140 K. It is well known that the structural phase transition is responsible for the dramatic change in the resistivity curve while the magnetic transition corresponds to the peak position in $d\rho(T)/dT$.[22] A neutron-scattering measurement[23] on polycrystalline NdFeAsO sample indicates T_{SDW}=141 K, being close to the peak temperature. The unusual decrease at about 8 K could be attributed to the ordering of the magnetic moment of Nd ions. The overall behavior of the resistivity is very similar to an earlier report on micrometer-sized NdFeAsO crystals.[24]

Figure 4 shows the temperature-dependent $R(\omega)$ and $\sigma_1(\omega)$ spectra of NdFeAsO. The energy gap features are not present above the structural transition (see spectra above 160 K). However, below the structural phase transition, the low-

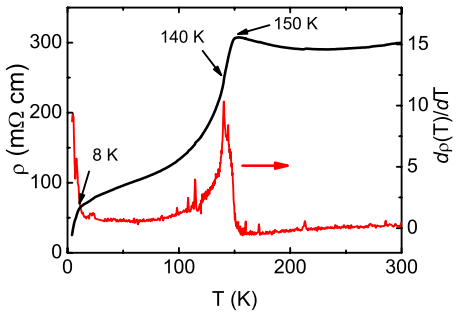

FIG. 3. (Color online) Temperature-dependent resistivity $\rho(T)$ and its derivative $d\rho(T)/dT$ curves for NdFeAsO. The strong anomaly near 150 K is linked to the structural transition, the sharp peak in $d\rho(T)/dT$ at 140 K corresponds to the magnetic transition. Another decrease near 8 K is attributed to the magnetic ordering of Nd moments.

frequency spectral-weight suppression appears. The spectral features observed at 142 K, a temperature between the structural and magnetic transitions, resemble to that at very low temperatures in the SDW state, although the features are weak at such a high temperature. This clearly indicates that the charge-excitation gaps start to open at the structural phase transition, thus demonstrating that the electronic state below but near the structural phase transition is already very close to that in the magnetic state. The observation would imply essentially the same driving mechanism for both transitions. Although the long-range magnetic order is not formed at the structural transition, short-range order, either nematic order or very strong spin fluctuations, would exist between the structural and magnetic transitions. We note that, a recent angle resolved photoemission spectroscopy experiment on a 111-based system NaFeAs, which also has separated structural and magnetic transitions, revealed band-

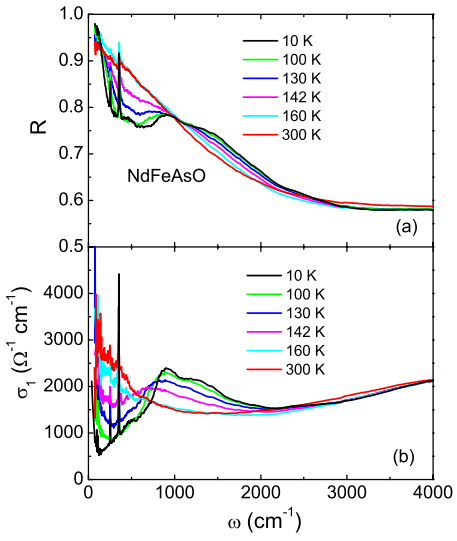

FIG. 4. (Color online) Reflectance and conductivity spectra of NdFeAsO at different temperatures. As temperature decreases from 300 to 160 K, a narrowing of Drude-type component is seen. However, a gaplike spectral-weight suppression at low frequencies is observed at 142 K, a temperature which is between the structural and the magnetic transitions.

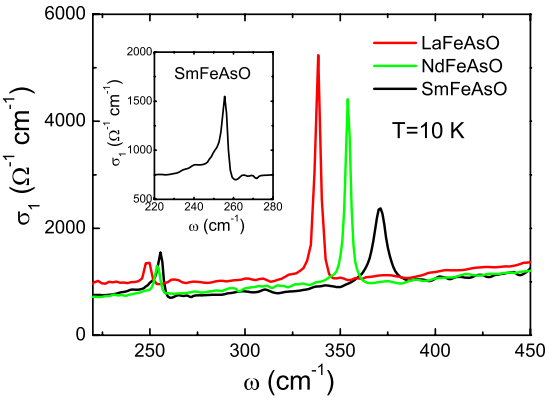

FIG. 5. (Color online) In-plane infrared phonon modes at 10 K for La-, Nd-, and Sm-based 1111 single crystals. Both the Fe-As and O-derived modes show hardening with the rare-earth element substitutions. Inset shows the expanded frequency region for Fe-As mode of SmFeAsO crystal. An asymmetric behavior is clearly seen, indicating strong electron-phonon coupling.

folding effect just below the structural transition;[25] while a NMR study on NaFeAs indicated strong enhancement of magnetic fluctuations.[26] Both are consistent with our optical measurement on 1111 systems.

C. Phonon spectra

Despite the fact that the electronic spectra display similar features for La or different rare-earth substituted 1111 parent compounds, we found that there exists a systematic frequency shift of infrared active in-plane phonon modes, which is the focus in the rest of the present paper. Figure 5 shows the low-frequency conductivity spectra of the *Re*FeAsO (*Re*=La, Nd, and Sm) crystals at 10 K, where two phonon modes could be seen in the frequency range. We shall show below that those phonon peaks do not show clear frequency shift across the structural and magnetic transitions.

It is known that *Re*FeAsO crystallizes in the tetragonal $P4/nmm$ structure at high temperature. According to symmetry analysis, there are six infrared active modes $3A_{2u}+3E_u$ along the c axis and in ab planes, respectively.[27] Early infrared reflectance measurement on polycrystalline LaFeAsO sample indicates five infrared active modes in the far-infrared region,[5] which could be assigned to those A_{2u} and E_u modes. Here we only observe two E_u modes at 248 and 339 cm^{-1} for LaFeAsO in the ab-plane response. It has to be noted that the 248 cm^{-1} mode seen in polycrystalline samples was assigned to the A_{2u} mode along the c axis in early studies while another mode with slightly higher frequency at 266 cm^{-1} was assigned to the in-plane E_u mode.[17,28] A comparison of the phonon modes between the single crystal and the polycrystalline samples indicates that the assignments of the two modes should be reversed. The 248 cm^{-1} E_u mode involves the in-plane displacement of Fe-As ions. The 339 cm^{-1} mode, which is particularly strong in intensity, is associated with the in-plane displacement of the O-La(*Re*) bonds. Its high-energy location indicates that this mode is mostly oxygen derived.[29] Several interesting features about the phonon modes are found from Fig. 5: (1)

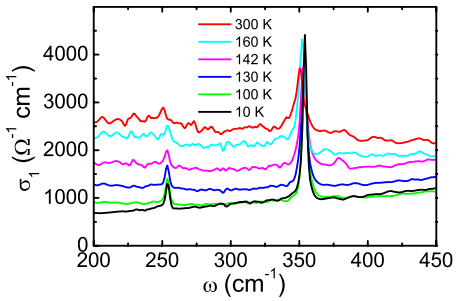

FIG. 6. (Color online) The temperature dependence of the in-plane phonon modes of NdFeAsO single crystal.

both in-plane E_u modes shift to higher frequencies in Nd- and Sm-based samples. The shift is more pronounced for the oxygen-derived mode. (2) The strength of Fe-As mode increases from LaFeAsO to NdFeAsO and SmFeAsO while the intensity of the O-*Re* (*Re*=La, Nd, and Sm) mode decreases. (3) There exist asymmetric line shapes for the phonon modes (Fano line shape[30]), evidencing sizable electron-phonon coupling effect. An expanded frequency plot for the Fe-As mode of SmFeAsO sample is shown in the inset of Fig. 5.

The increase in the phonon frequency in rare-earth element substituted systems strongly indicates an enhancement of the in-plane Fe-As and O-*Re* bonding strengths. With the substitution of La by Nd and Sm, the masses of the rare-earth ions increase. If there were no bonding strength change, we would expect a reduction in frequencies of the in-plane O-*Re* stretching mode. The noticeable increase in the mode frequency suggests a reduction in the bond length, and it overcomes the effect of the mass change in the rare-earth ions. Not only the O-derived mode shows a substantial increase, but the in-plane Fe-As mode also shows a hardening from LaFeAsO to NdFeAsO and SmFeAsO, although less pronounced. It is worth noting that the Raman-scattering measurements also indicate a strong hardening of the Raman active O mode.[27,28] Overall, the observations are consistent with the structural characterization data which show a decreasing of the Fe-As bond length.[8,9]The above result is not affected by the F doping, since low-level F doping is found to have little influence on the phonon frequencies of the parent compound.[31]

Figure 6 shows the temperature evolution of the E_u phonon modes across the structural and magnetic transitions for the prototype NdFeAsO crystal. Similar to the case of infrared measurement on the polycrystalline samples,[5] we do not observe any splitting or new phonon lines below the structural transition. According to density-functional theory calculations on LaFeAsO, the splitting of the infrared active phonon modes would be very small and therefore could not be well resolved by the optical measurement.[17] The intensities of the two modes show significant temperature dependence. They are strongly enhanced below the structural or magnetic transition. This behavior is similar to the observation in $BaFe_2As_2$ crystal where two infrared active in-plane modes near 94 and 253 cm^{-1} are observed, and the 253 cm^{-1} mode shows a strong intensity enhancement below the structural transition. A natural explanation is that the screening effect from the conduction electrons is significantly reduced due to the partial gapping of Fermi surfaces. Alternatively, it was proposed that the intensity change could be due to a charge redistributions at each atom leading to a change in bonding between different atoms.[32] This point of view might be useful in interpreting the intensity increase in the Fe-As stretching mode but the decrease in the O-La mode from LaFeAsO to NdFeAsO and SmFeAsO.

The above experimental results indicate a good correlation between the reduction in the bond length in the crystal structure and the increase in the infrared phonon mode frequencies. Since the rare-earth element substitutions for La significantly enhance the superconducting transition temperature in doped compounds, it is of worth to further investigate the role played by the electron-phonon coupling for the superconductivity.

III. CONCLUSIONS

We have grown single crystals of the parent compounds LaFeAsO, NdFeAsO, and SmFeAsO by means of a NaAs flux growth technique and studied their charge excitations and infrared phonon spectra by optical spectroscopy measurement. We identify that the charge-excitation gaps are already present below the structural phase transition with spectral feature similar to those found at the SDW state, thus illustrating that the electronic state below the structural phase transition is essentially the same as that in the SDW state. We show that in-plane infrared phonon modes display noticeable shifts toward high frequency upon rare-earth element (Nd and Sm) substitutions for La, indicating a strong enhancement of the bonding strength. The observation is well correlated with the reduction in the bond length in Nd- and Sm-based systems. The study also yields evidence for the presence of electron-phonon coupling effect in the compounds.

ACKNOWLEDGMENTS

We thank P. Dai, J. L. Luo, and T. Xiang for useful discussions. This work was supported by the National Science Foundation of China, the Knowledge Innovation Project of the Chinese Academy of Sciences, and the 973 project of the Ministry of Science and Technology of China.

[1] Y. Kamihara, T. Watanabe, M. Hirano, and H. Hosono, J. Am. Chem. Soc. **130**, 3296 (2008).
[2] G. F. Chen, Z. Li, D. Wu, G. Li, W. Z. Hu, J. Dong, P. Zheng, J. L. Luo, and N. L. Wang, Phys. Rev. Lett. **100**, 247002 (2008).
[3] Z. A. Ren, J. Yang, W. Lu, W. Yi, X. L. Shen, Z. C. Li, G. C. Che, X. L. Dong, L. L. Sun, F. Zhou, and Z. X. Zhao, EPL **82**, 57002 (2008).
[4] Z.-A. Ren, W. Lu, J. Yang, W. Yi, X.-L. Shen, Z. C. Li, G.-C. Che, X.-L. Dong, L.-L. Sun, F. Zhou, and Z.-X. Zhao, Chin. Phys. Lett. **25**, 2215 (2008).
[5] J. Dong, H. J. Zhang, G. Xu, Z. Li, G. Li, W. Z. Hu, D. Wu, G. F. Chen, X. Dai, J. L. Luo, Z. Fang, and N. L. Wang, EPL **83**, 27006 (2008).
[6] C. de la Cruz, Q. Huang, J. W. Lynn, J. Li, W. Ratcliff II, J. L. Zarestky, H. A. Mook, G. F. Chen, J. L. Luo, N. L. Wang, and P. Dai, Nature (London) **453**, 899 (2008).
[7] L. Boeri, O. V. Dolgov, and A. A. Golubov, Phys. Rev. Lett. **101**, 026403 (2008).
[8] J. Zhao, Q. Huang, C. de la Cruz, S. Li, J. W. Lynn, Y. Chen, M. A. Green, G. F. Chen, G. Li, Z. Li, J. L. Luo, N. L. Wang, and P. Dai, Nature Mater. **7**, 953 (2008).
[9] C. H. Lee, A. Iyo, H. Eisaki, H. Kito, M. T. Fernandez-Diaz, T. Ito, K. Kihou, H. Matsuhata, M. Braden, and K. Yamada, J. Phys. Soc. Jpn. **77**, 083704 (2008).
[10] N. D. Zhigadlo, S. Katrych, Z. Bukowski, S. Weyeneth, R. Puzniak, and J. Karpinski, J. Phys.: Condens. Matter **20**, 342202 (2008).
[11] H.-S. Lee, J.-H. Park, J.-Y. Lee, J.-Y. Kim, N.-H. Sung, T.-Y. Koo, B. K. Cho, C.-U. Jung, S. Saini, S.-J. Kim, and H.-J. Lee, Supercond. Sci. Technol. **22**, 075023 (2009).
[12] J.-Q. Yan, S. Nandi, J. L. Zarestky, W. Tian, A. Kreyssig, B. Jensen, A. Kracher, K. W. Dennis, R. J. McQueeney, A. I. Goldman, R. W. McCallum, and T. A. Lograsso, Appl. Phys. Lett. **95**, 222504 (2009).
[13] Z. G. Chen, R. H. Yuan, T. Dong, and N. L. Wang, Phys. Rev. B **81**, 100502(R) (2010).
[14] R. Pöttgen and D. Johrendt, Z. Naturforsch. **63b**, 1135 (2008).
[15] W. Z. Hu, J. Dong, G. Li, Z. Li, P. Zheng, G. F. Chen, J. L. Luo, and N. L. Wang, Phys. Rev. Lett. **101**, 257005 (2008).
[16] W. Z. Hu, G. Li, P. Zheng, G. F. Chen, J. L. Luo, and N. L. Wang, Phys. Rev. B **80**, 100507(R) (2009).
[17] T. Yildirim, Phys. Rev. Lett. **101**, 057010 (2008); Physica C **469**, 425 (2009).
[18] F. J. Ma, Z. Y. Lu, and T. Xiang, Phys. Rev. B **78**, 224517 (2008).
[19] C. Fang, H. Yao, W.-F. Tsai, J. P. Hu, and S. A. Kivelson, Phys. Rev. B **77**, 224509 (2008).
[20] C. Xu, M. Muller, and S. Sachdev, Phys. Rev. B **78**, 020501(R) (2008).
[21] G.-F. Chen, Z. Li, D. Wu, J. Dong, G. Li, W.-Z. Hu, P. Zheng, J.-L. Luo, and N.-L. Wang, Chin. Phys. Lett. **25**, 2235 (2008).
[22] M. A. McGuire, A. D. Christianson, A. S. Sefat, B. C. Sales, M. D. Lumsden, R. Jin, E. A. Payzant, D. Mandrus, Y. Luan, V. Keppens, V. Varadarajan, J. W. Brill, R. P. Hermann, M. T. Sougrati, F. Grandjean, and G. J. Long, Phys. Rev. B **78**, 094517 (2008).
[23] Y. Chen, J. W. Lynn, J. Li, G. Li, G. F. Chen, J. L. Luo, N. L. Wang, P. Dai, C. de la Cruz, and H. A. Mook, Phys. Rev. B **78**, 064515 (2008).
[24] P. Cheng, H. Yang, Y. Jia, L. Fang, X. Zhu, G. Mu, and H. H. Wen, Phys. Rev. B **78**, 134508 (2008).
[25] C. He, Y. Zhang, B. Xie, X. Wang, L. Yang, B. Zhou, F. Chen, M. Arita, K. Shimada, H. Namatame, M. Taniguchi, X. Chen, J. Hu, and D. Feng, arXiv:1001.2981 (unpublished).
[26] Yu. Weiqiang, L. Ma, J. Zhang, G. Chen, T. Xia, S. Zhang, and Y. Hou, arXiv:1004.3581 (unpublished).
[27] V. G. Hadjiev, M. N. Iliev, K. Sasmal, Y.-Y. Sun, and C. W. Chu, Phys. Rev. B **77**, 220505(R) (2008).
[28] C. Marini, C. Mirri, G. Profeta, S. Lupi, D. Di Castro, R. Sopracase, P. Postorino, P. Calvani, A. Perucchi, S. Massidda, G. M. Tropeano, M. Putti, A. Martinelli, A. Palenzona, and P. Dore, EPL **84**, 67013 (2008).
[29] D. J. Singh and M.-H. Du, Phys. Rev. Lett. **100**, 237003 (2008).
[30] U. Fano, Phys. Rev. **124**, 1866 (1961).
[31] L. Zhang, T. Fujita, F. Chen, D. L. Feng, S. Maekawa, and M. W. Chen, Phys. Rev. B **79**, 052507 (2009).
[32] A. Akrap, J. J. Tu, L. J. Li, G. H. Cao, Z. A. Xu, and C. C. Homes, Phys. Rev. B **80**, 180502(R) (2009).